Urol Res (1994) 22:209–212

ORIGINAL PAPER

C. Dawson · K. Aitken · Y. Ng · G. Dolke · D. Gadian
H. N. Whitfield

Magnetic resonance imaging of urinary calculi

Received: 24 August 1993 / Accepted: 26 November 1993

Abstract Accurate prediction of the response of an individual patient to lithotripsy remains impossible. Certain factors such as the chemical composition, size, and position of the calculus are known to be important in determining the success rate. This paper reports the use of magnetic resonance imaging (MRI) to evaluate 141 urinary calculi in vitro. A wide range of signals for each chemical type of calculus was found on each of the three imaging sequences used (T1-weighted, T2-weighted, and proton density). None of the chemical groups examined showed a typical MRI profile allowing it to be distinguished from the other groups. Analysis of variance showed a statistical difference between signals for apatite and struvite on the T1-weighted sequence, and between struvite and uric acid on the proton density sequence (both, $P < 0.05$). These results show for the first time that MRI is capable of distinguishing between different chemical types of stones. This is particularly important for the comparison of struvite and apatite which appear to be similar in conventional investigations but have quite different hardness values. Further work is in progress correlating the results of this study with stone microhardness and extracorporeal shockwave lithotripsy fragility tests to determine whether MRI accurately predicts the success of lithotripsy.

Key words Extracorporeal shockwave lithotripsy · Magnetic resonance imaging · Stone hardness

C. Dawson (✉) · H. N. Whitfield
Department of Urology, Battle Hospital,
Oxford Road, Reading RG3 1AG, UK

Y. Ng · G. Dolke
Department of Diagnostic Radiology,
St. Bartholomew's Hospital,
London, UK

K. Aitken · D. Gadian
MRI Department, Hospitals for Sick Children,
Great Ormond St. London, UK

Accurate prediction of response to lithotripsy remains a challenge for the urologist. The size of the stone and its location are known to be important factors in determining the success rate, as is the chemical composition. Knowledge of the stone composition is important because urate, calcium oxalate monohydrate (whewellite), and cystine stones are hard stones and less responsive to treatment with extracorporeal shockwave lithotripsy (ESWL). Analysis of urine before lithotripsy using either scanning electron microscopy or X-ray dispersive spectroscopy has been shown to identify the chemical composition of stones with 100% accuracy [3]. Knowledge of the composition of previous stones suffered by the patient is useful, but does not necessarily mean that further stones will be of the same composition; furthermore, it does not give any indication of the success of lithotripsy in any given patient.

Magnetic resonance (MR) spectroscopy has been in use in vitro since 1945. With the development of advanced computer technology, imaging with MR has become increasingly sophisticated. Magnetic resonance imaging (MRI) has been used to study gallstones [2, 4] in vitro. The literature to date on MRI of renal calculi is sparse. In this in vitro study we have evaluated the MR appearances of 141 renal calculi to assess whether it is possible to distinguish stones of different chemical composition on MRI.

Materials and methods

One hundred and forty one renal calculi, ranging in size from 4 to 68 mm (mean 21.3 mm), were all rehydrated fully in saline under a gentle vacuum for 48 h prior to scanning. MRI was performed using a 1.5 T machine (Siemens Magnetom). The stones (in their saline-filled pots) were placed in a phantom within a circularly polarised head coil with a field of view (FOV) of 30 cm. Six pots were scanned at a time. Images were taken using the following sequences: T1-weighted (TR 600 ms, TE 15 ms); T2-weighted (TR 2500 ms, TE 90 ms); proton density (TR 2500 ms, TE 20 ms), where TR = repetition time, and TE = echo time.

A slice thickness of 3 mm with a FOV of 16.5 cm was used for each sequence. Images were recorded on film using a 256 × 256 matrix for

Table 1 Number of calculi determined by infrared spectroscopy

	Number scanned by MRI
Calcium oxalate	81
Apatite	22
Magnesium, ammonium, phosphate	18
Uric acid	14
Ammonium urate	4
Sodium urate	1
Cystine	1
Total	141

the T1-weighted sequences, and a 160×256 matrix for the T2-weighted and proton density sequences.

The signal intensity of each stone was recorded from the computer monitor using software designed for the MR scanner. With the image in view a circular cursor was placed over the region of interest, and the signal sampled. The signal from the stones was compared with the background signal and with a saline control. This was done without knowledge of the chemical composition of the stones, which had been determined prior to MRI using infrared spectroscopy.

Results

On the basis of the infrared spectroscopy, the stones were separated into the following groups for the analysis of results; calcium oxalate (both mono- and dihydrate), uric acid, magnesium ammonium phosphate, apatite, ammonium urate, sodium urate, and cystine. Table 1 shows the number of stones in each group.

The range, mean and standard error of the signal intensities for all stones (grouped by chemical composition) for each of the three sequences are shown in Table 2. Figure 1 shows the range and mean signals obtained on the T1-weighted sequence for eac h of the chemical groups. There was a wide range in signal intensity for each chemical type on all sequences (Figs. 1–3).

For each sequence the distribution of signal intensities was skewed towards the lower end of the range. Therefore the data were recalculated using the log to the base 10 ($\log_{10}$) in order to "normalise" the data. Statistical analysis was performed using the Kruskal-Wallace test, which is equivalent to the one-way analysis of variance test (ANOVA) for non-parametric data. Only data for uric acid, calcium oxalate, struvite, and apatite stones were included in this analysis because the other groups contained too few examples. All stones produced signals which differed significantly from saline, on each of the three sequences ($P < 0.05$). In addition, struvite differed significantly from apatite on the T1 sequence ($0.05 > P > 0.01$), and uric acid differed from struvite on the proton density sequence ($0.05 > P > 0.01$). No statistical difference was found between any of the groups on the T2 sequence.

Table 2 Mean, and range of values for each group and sequence

	T1-weighted sequence	Signal	T2-weighted sequence	Signal	Proton density sequence	Signal
Calcium oxalate	Count	81.00	Count	81.00	Count	80.00
	Minimum	−2.60	Minimum	−10.80	Minimum	−2.70
	Maximum	540.70	Maximum	613.50	Maximum	876.40
	Range	543.30	Range	624.30	Range	879.10
	Mean	72.58	Mean	59.94	Mean	154.26
	Standard error	10.09	Standard error	12.76	Standard error	20.61
Apatite	Count	22.00	Count	22.00	Count	22.00
	Minimum	−0.70	Minimum	− 7.10	Minimum	−2.10
	Maximum	192.70	Maximum	346.90	Maximum	590.10
	Range	193.40	Range	354.00	Range	592.20
	Mean	40.12	Mean	44.18	Mean	133.97
	Standard error	12.14	Standard error	19.22	Standard error	39.81
Magnesium ammonium phosphate (struvite)	Count	18.00	Count	18.00	Count	19.00
	Minimum	0.80	Minimum	3.00	Minimum	5.30
	Maximum	187.40	Maximum	543.30	Maximum	693.40
	Range	186.60	Range	540.30	Range	688.10
	Mean	79.09	Mean	87.67	Mean	228.43
	Standard error	14.45	Standard error	35.77	Standard error	48.99
Uric acid	Count	14.00	Count	13.00	Count	14.00
	Minimum	5.50	Minimum	−16.20	Minimum	3.90
	Maximum	227.70	Maximum	97.30	Maximum	284.40
	Range	221.70	Range	113.50	Range	280.50
	Mean	47.42	Mean	20.76	Mean	82.67
	Standard error	15.62	Standard error	8.83	Standard error	22.01
Ammonium urate	Count	4.00	Count	4.00	Count	4.00
	Minimum	13.80	Minimum	0.80	Minimum	8.00
	Maximum	212.10	Maximum	280.00	Maximum	629.20
	Range	198.30	Range	279.20	Range	621.20
	Mean	65.65	Mean	84.55	Mean	190.18
	Standard error	48.84	Standard error	66.30	Standard error	146.89

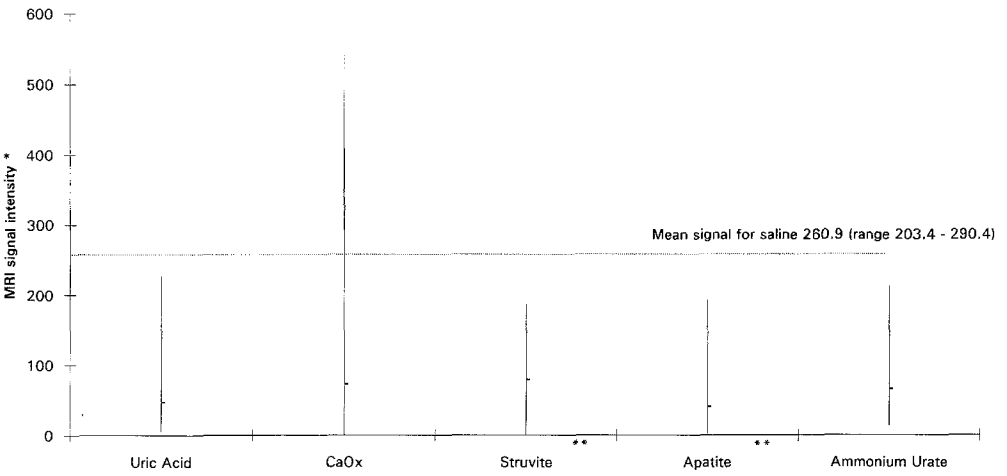

Fig. 1 MRI signals for T1-weighted sequence. Length of line represents range of signals. Mean signal intensity shown by *horizontal bar*. *Signal intensities have been corrected for background signal; **statistically signifant difference

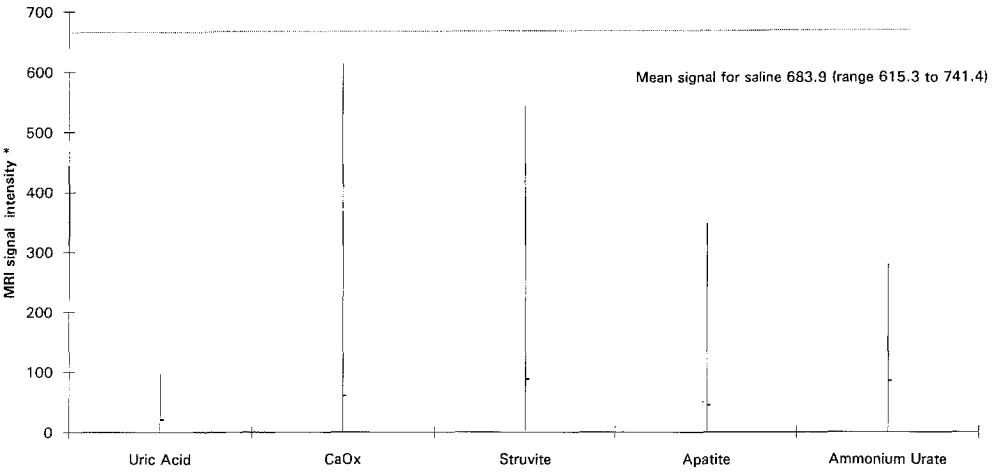

Fig. 2 MRI signals for T2-weighted sequence. Length of line represents range of signals; mean signal intensity shown by *horizontal bar*. *Signal intensities have been corrected for background signal

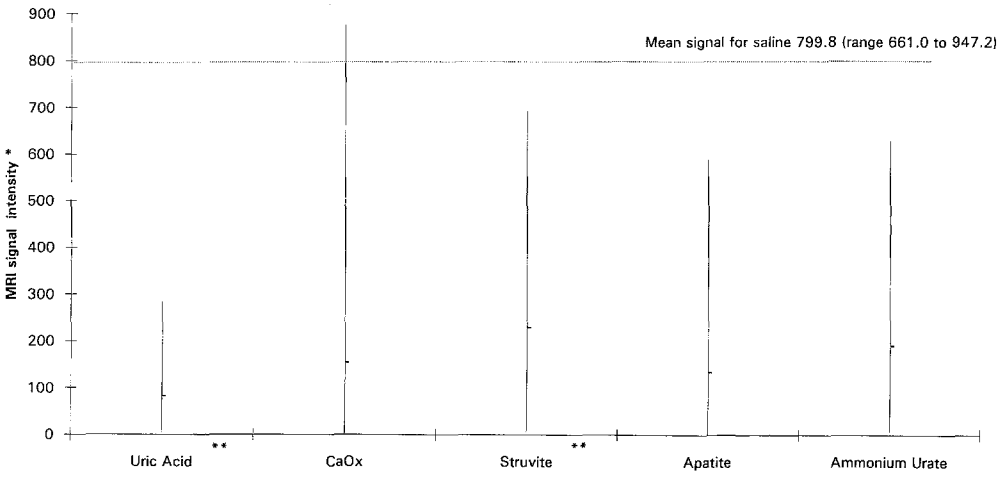

Fig. 3 MRI signals for proton density sequence. Length of line represents of signals; mean signal intensity shown by *horizontal bar*. *Signal intensities have been corrected for background signal; **statistically significant difference

Discussion

MRI is non-invasive, does not use ionising radiation, and is without known hazards [1]. These properties make it both an attractive research tool and render it particularly suitable for in vivo use. Little has been written concerning the MRI characteristics of renal calculi. Stoller et al. [5] examined 20 urinary calculi using a 1.5 T Signa system, but were unable to differentiate calculi on the basis of the grey scale images produced. They found that, as predicted for solid material, most of the stones showed near complete absence of signal intensity on each of the sequences used, and where a signal was seen this was found to be due to partial volume effects. In a pilot study preceding the current study we looked at 20 urinary calculi by MRI using similar sequences to Stoller et al. and were unable to distinguish calculi using the grey scale method. Therefore

we abandoned this method of data analysis and have chosen instead to record the signal intensities.

Chemical analysis of stones may be performed by various methods. Optical crystallography, as used by Stoller et al., is limited by expertise. Apatite does not have a typical crystal appearance using this method and often appears as indeterminate granules, and oxalate can appear quite different to the classic envelope-shaped crystals described in textbooks. We used infrared spectroscopy (IRS) which is quick, simple to use, and gives sensitive and reproducible results with the minimum of training. As with all methods of analysis, the results of IRS are only as good as the sample provided. The calculi in this study were received intact and samples were provided for IRS by shaving a small sample from the external surface using a razor blade, leaving the rest of the calculus for both MRI and further tests. Thus it is possible that some adjustment of the chemical groups may be necessary when the stones have been fragmented on the lithotripter.

Our results differ markedly from those of Stoller et al. and show for the first time that MRI is capable of distinguishing between groups of urinary calculi, although solids are known to exhibit low-intensity MRI signals. The T1-weighted sequence successfully distinguished struvite calculi from apatite, whilst struvite was seen to differ significantly from uric acid on the proton density sequence. None of the groups investigated showed a typical MRI profile enabling differentiation from the other groups. Uric acid stones are radiolucent on intravenous urography and may therefore be detected without resorting to MRI, but the ability to differentiate struvite stones from apatite stones is important because they appear similar on conventional investigations, although their hardness is very different.

Further studies are in progress to establish the relationship of these results to stone hardness (as determined by in vitro microhardness and ESWL fragility) in order to ascertain whether these preliminary findings will enable us to use MRI in vivo to predict which stones would be suitable for lithotripsy.

References

1. Andrew ER (1982) Nuclear magnetic resonance imaging. In: Wells PNT (ed) Scientific basis of medical imaging. Churchill Livingstone, Edinburgh, p 212
2. Baron RL, Shuman WP, Lee SP et al. (1989) MR appearance of gallstones in vitro at 1.5 T: correlation with chemical composition. AJR 153:497
3. Cohen NP, Parkhouse H, Scott ML et al. (1992) Prediction of response to lithotripsy: the use of scanning electron microscopy and x-ray energy dispersive spectroscopy. Br J Urol 70:469
4. Moon KL, Hricak H, Margolis AR et al. (1983) Nuclear magnetic resonance imaging characteristics of gallstones in vitro. Radiology 148:753
5. Stoller MI, Floth A, Hricak H et al. (1991) Magnetic resonance imaging of renal calculi: an in vitro study. J Lithotripsy Stone Dis 3:162